ACS APPLIED MATERIALS & INTERFACES

Research Article

www.acsami.org

Dextrin and Poly(acrylic acid)-Based Biodegradable, Non-Cytotoxic, Chemically Cross-Linked Hydrogel for Sustained Release of Ornidazole and Ciprofloxacin

Dipankar Das,[†] Paulomi Ghosh,[‡] Santanu Dhara,[‡] Asit Baran Panda,[§] and Sagar Pal*[,†]

[†]Polymer Chemistry Laboratory, Department of Applied Chemistry, Indian School of Mines, Dhanbad 826004, India

[‡]Biomaterials and Tissue Engineering Laboratory, School of Medical Science and Technology, Indian Institute of Technology Kharagpur 721302, India

[§]Discipline of Inorganic Materials and Catalysis, Central Salt and Marine Chemicals Research Institute (CSIR), Bhavnagar 364002, Gujarat, India

Supporting Information

ABSTRACT: Herein, novel biodegradable, stimulus-responsive, chemically cross-linked and porous hydrogel has been synthesized to evaluate its applicability as an efficient carrier for sustained release of ornidazole and ciprofloxacin. The cross-linked hydrogel (c-Dxt/pAA) has been developed from dextrin and poly(acrylic acid) using *N*,*N*′-methylene bis(acrylamide) cross-linker via Michael-type addition reaction. With the variation of reaction parameters, various c-Dxt/pAA hydrogels have been synthesized to optimize the best one. c-Dxt/pAA hydrogel has been characterized using various physicochemical characterization techniques. The hydrogel demonstrates significant pH and temperature sensitivity. Gel characteristics and gel kinetics have been performed through the measurement of rheological parameters. The hydrogel shows noncytotoxic behavior toward human mesenchymal stem cells. Biodegradation study predicts that c-Dxt/pAA is degradable in nature. The in vitro release of ornidazole and ciprofloxacin suggests that the hydrogel released both the drugs in a controlled manner with extensive stability up to 3 months. The results suggest that c-Dxt/pAA is probably a promising candidate for controlled release of ornidazole and ciprofloxacin.

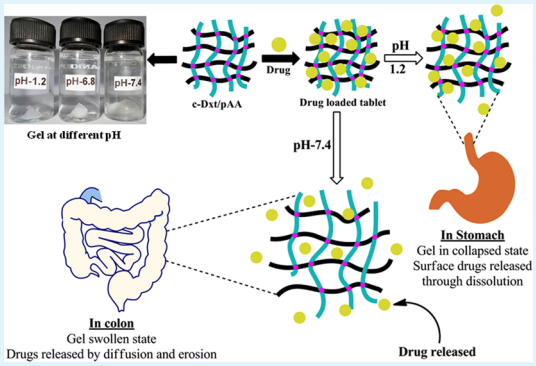

KEYWORDS: *biodegradable, dextrin, hydrogel, poly(acrylic acid), drug delivery*

1. INTRODUCTION

Drug delivery systems that are proficient for the controlled release of multiple drugs have become significant in recent years for their ability to deliver drugs in a predetermined rate and to optimize the therapeutic effects.[1−3] Controlled-release drug delivery system released the drug into the body at a definite rate in response to stimuli or time.[2] Over the past decade, porous polymeric hydrogels have been used extensively as carriers for sustained/delayed drug release, where the rate of release is controlled by diffusion process or by combination of diffusion and erosion of the matrix.[4,5] Recently, stimuli-responsive gels have drawn significant attention in drug delivery application.[6−8] These gels can exhibit phase transitions in response to various stimuli including pH,[9,10] temperature,[11] light,[12] electric field,[13] magnetic field,[14] and so on. Besides, the stimuli-responsive gels demonstrate several striking properties such as defined morphology, high porosity, adjustable dimensions, resemblance with soft tissues, and the ability of their network to absorb large amount of water. These properties make the hydrogels promising candidates for potential biomedical application.[15−17]

Hydrogels are physically or chemically cross-linked, insoluble, three-dimensional, hydrophilic polymers that can swell by absorbing excess amount of water in the presence of aqueous solution or biological fluids.[9,18] The excellent swelling characteristics of the hydrogel favors the retention of more water that helps in maintaining excellent blood compatibility, structural integrity, and elasticity.[7] Hydrogels have been used in various biomedical applications such as tissue engineering,[19,20] cell-based biosensors,[21] coatings,[22] drug delivery,[9,18,23] packers in oil and gas recovery,[24] and cell transplantation.[25] pH responsive physically or chemically cross-linked hydrogels have also been investigated as controlled drug delivery matrix because of their admirable sustained release characteristics, which can be tuned by their pH-dependent swelling behavior.[7] Compared to physically cross-linked hydrogels, chemically cross-linked hydrogels have better mechanical strength and gel characteristics.[26,27] But the pharmaceutical applications of chemically cross-linked hydrogels are limited, owing to the

Received: December 10, 2014
Accepted: February 5, 2015
Published: February 5, 2015

DOI: 10.1021/am508712e
ACS Appl. Mater. Interfaces 2015, 7, 4791−4803

toxic nature of cross-linkers.[26,27] Thus, one of the greatest challenges in drug delivery is to develop novel chemically cross-linked hydrogels that are efficient and should be biocompatible. Besides, better mechanical strength, higher degree of swelling, and stimulus responsive behavior makes the hydrogels superior bioadhesive materials.[28]

Our interest lies in exploring the development of a novel chemically cross-linked, biodegradable and biocompatible hydrogel for controlled drug delivery application. Modified polysaccharide-based physically cross-linked hydrogels/composites have already been used for drug delivery applications.[4,9,18,26,29−31] However, for the pharmaceutical requirements like better bioavailability of drugs, good compatibility between the drug and hydrogel, noncytotoxicity of the gel and sufficient drug stability in tablet formulations, controlled release of multiple drugs from chemically cross-linked hydrogels are far less studied. Polymers synthesized from natural or synthetic sources having hydroxyl, amine, amide, ether, and sulfonate groups in their side chains, are used for developing chemically cross-linked hydrogels, and might be suitable for both hydrophilic and hydrophobic drug molecules.[6]

Herein, we have designed and prepared a stimulus-responsive chemically cross-linked hydrogel (c-Dxt/pAA) derived from dextrin as biopolymer, MBA as cross-linker and acrylic acid as monomer for sustained release of model drugs ornidazole and ciprofloxacin. The polymerization process and cross-linking phenomenon have been explained using ^{1}H-nuclear magnetic resonance (NMR) spectra. The ^{1}H NMR spectra also showed that the sp^2 hybridized carbon atoms of cross-linker (MBA) was converted to sp^3 hybridized carbon atoms during cross-linking reaction, thereby eradicating the cross-linker's toxicity in the cross-linked hydrogel. This would open a new pathway for the use of chemically cross-linked hydrogel in the biomedical field. It is worth mentioning that dextrin is a natural biopolymer with a high degree of efficacy for the development of cross-linked hydrogels owing to its natural abundance, presence of functional hydroxyl groups, low cost, and excellent biocompatibility and biodegradability.[32] On the other hand, acrylic acid can play an important role for stimuli-responsiveness and bioadhesive characteristics because of the presence of −COOH groups in their chain,[28] the developed chemically cross-linked hydrogel (in the presence of MBA cross-linker) seems to be a potential candidate for the controlled release of ornidazole and ciprofloxacin.

The developed hydrogel demonstrated unique characteristics such as (a) stimulus responsive behavior, which is significant in drug release applications, and (b) adequate gel strength due to covalent attachment of cross-linker. As a result, it can prevent the dissolution phenomena during drug delivery and minimize the erosion rate, which controls the release pattern. More significantly, the noncytotoxicity and biodegradability of c-Dxt/pAA are the major concerns for real life applications. Because of its sufficient gel stability, stimulus-responsiveness and porous structure, c-Dxt/pAA delivers two different types of drugs (colon specific and antibiotic) in a more sustained way with excellent stability up to 3 months. These characteristics imply that c-Dxt/pAA hydrogel could be a promising alternative for the controlled delivery of both ornidazole and ciprofloxacin.

2. EXPERIMENTAL SECTION

2.1. Chemicals. Dextrin (Fluka, Switzerland); *N*,*N*′-methylene bis(acrylamide) (MBA; Loba Chemie, Pvt., Ltd., Mumbai, India); potassium persulfate (KPS; GlaxoSmithKline Pharmaceuticals, Ltd., Mumbai, India); acrylic acid (AAc), acetone and methanol (E-Merck (I), Pvt., Ltd., Mumbai, India); ornidazole (gift sample from Endoc Pharma, Rajkot, India); ciprofloxacin (Sigma-Aldrich, Germany); polyvinylpyrrolidone (PVP-K30; Spectrochem, Pvt., Ltd., Mumbai, India) were used as received. Lysozyme hydrochloride from egg white was purchased from TCI, Pvt., Ltd., Tokyo, Japan.

2.2. Synthesis of Cross-Linked Hydrogel. The c-Dxt/pAA hydrogel was synthesized via free radical polymerization in presence of KPS initiator. A typical experimental process is given below:

One gram (6.2×10^{-3} moles) of dextrin was dissolved in distilled water (80 mL) in a three-neck round bottom flask. The flask was fitted with a magnetic stirrer and placed in an oil bath at 50 °C, with stirring speed of 400 rpm. Argon gas was purged into the flask to create inert atmosphere. After 10 min, aqueous solution of KPS, requisite amount of acrylic acid (AAc; see Table 1) were added separately into the dextrin solution. Subsequently, the reaction temperature was raised to 70 °C. Once the solution appeared relatively viscous, cross-linker was added. The copolymerization reaction continued at same temperature for 3 h. The polymerization reaction was terminated using 5 mL (0.1 v/w %) saturated hydroquinol solution.

The resultant product (probably a mixture of hydrogel, homopolymer, unreacted monomer, and cross-linker) was cooled to room temperature and dispersed in methanol/water (70:30) mixture overnight. After that, the product was washed with acetone to remove poly(acrylic acid) (i.e., homopolymer) and unreacted monomer as well as cross-linker from the mixture. Finally, the gel-like mass (i.e., pure c-Dxt/pAA hydrogel, free from any homopolymer as well as unreacted monomer) was dried in a vacuum oven at 40 °C, until the constant mass was obtained. The dried hydrogel (i.e., c-Dxt/pAA xerogel) was used for various characterizations and controlled release application.

2.3. Characterization. FTIR spectra of dextrin, c-Dxt/pAA 8 xerogel, ornidazole, ciprofloxacin drugs and corresponding tablets were performed in solid state (KBr pellet method). The spectrum of acrylic acid was recorded using DCM solvent (Model IR-PerkinElmer, Spectrum 2000).

C, H, N analysis was carried out using Elemental Analyzer (Vario EL III, Elementar, Germany).

Solid state ^{13}C NMR spectrum of c-Dxt/pAA 8 xerogel was recorded at 500 MHz on a Bruker Advance II-500 NMR spectrophotometer. Liquid state ^{1}H NMR spectra were recorded using DMSO-d_6 solvent in swollen state at 400 MHz using Bruker spectrophotometer.

Thermogravimetric analyses of dextrin and c-Dxt/pAA 8 xerogel were performed using TGA analyzer (STA449F3, Netzsch, Germany) with inert atmosphere of N_2. Heating rate was maintained at 5 °C/min.

Solid state UV−vis-NIR study was performed using Cary series UV−vis−NIR Spectrophotometer (Cary 5000).

The surface morphologies of dextrin, c-Dxt/pAA 8 xerogel were investigated using field emission scanning electron microscopy (FESEM Supra 55, Zeiss, Germany). In addition, the surface morphology of the c-Dxt/pAA 8 hydrogel at swollen state (aqueous media using pH 7.4 buffer) was performed by environmental scanning electron microscopy (E-SEM; EVO 18, Zeiss, Germany).

2.4. Rheological Characteristics. Rheological assessments of dextrin and c-Dxt/pAA hydrogels were performed in swollen state at pH 7.4 using a rheometer (Bohlin Gemini-2, Malvern, United Kingdom). Oscillatory sweep measurement was performed with constant frequency of 1 Hz and in different shear stress in the range of 1−100 Pa using parallel plate geometry. The fixed tool gap was 500 μm. The rheological characteristics of swollen c-Dxt/pAA hydrogels were determined in PBS media, pH 7.4 after attaining equilibrium swelling (~13 h) at 37 °C. The frequency sweep measurement of hydrogel was performed in the range of 1−10 Hz with a constant stress of 30 Pa at 37 and 70 °C. The shear viscosity of the c-Dxt/pAA 8 hydrogel was evaluated at different shear rates ranging from 0.1 to 1000 s^{-1} at 37 °C. Further, the elastic (G') and loss (G'') modulii of hydrogels were measured at 37 and 70 °C to calculate the gel strength.[33] The gelation time[34] of c-Dxt/pAA 8 hydrogel was determined by investigating the dynamic time sweep (0−30 min)

DOI: 10.1021/am508712e
ACS Appl. Mater. Interfaces 2015, 7, 4791−4803

Scheme 1. Probable Mechanism for Synthesis of c-Dxt/pAA Hydrogel

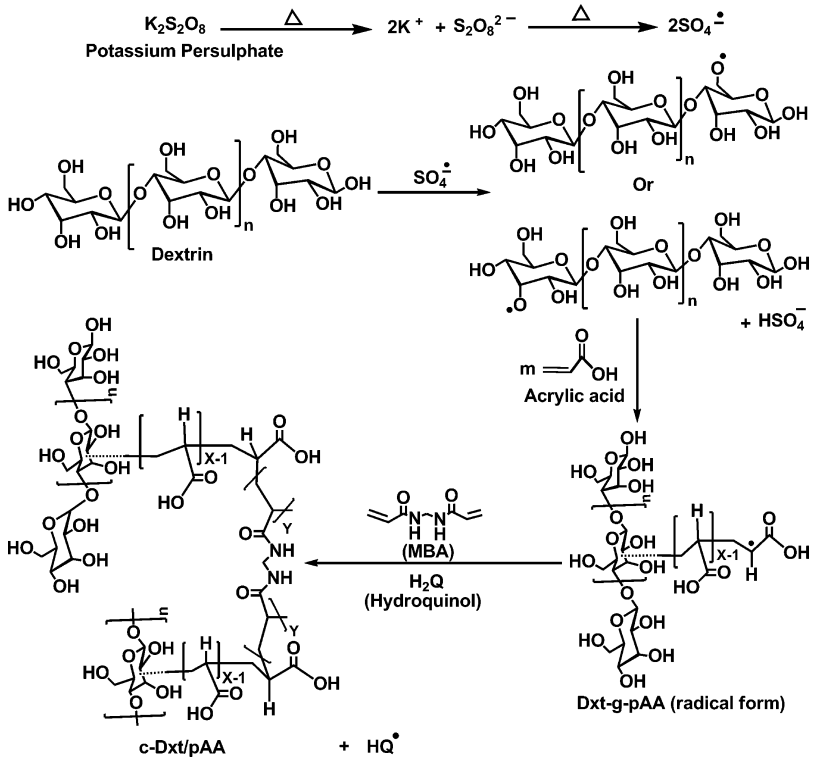

and dynamic frequency sweep measurements (0.5−3.0 Hz) at various cure times with parallel plate geometry at the reaction temperature (i.e., 70 °C).

2.5. Biodegradation Study Using Hen Egg Lysozyme. The biodegradation test of c-Dxt/pAA 8 xerogel film was investigated using hen egg lysozyme as reported in literature.[35−37] The preweighted c-Dxt/pAA 8 xerogel films (10 × 10 × 0.1 mm) were immersed in 2 mL of buffer (pH 7) solution that had the enzyme lysozyme at a natural concentration, as observed within the human body (1.5 $\mu g/mL^{-1}$). The temperature of the study was maintained at 37 °C. After regular time period, the films were collected from the solution, washed with distilled water and reweighted.[35] The degree of in vitro biodegradation was represented as % weight loss with time. For the comparison study, another film was also immersed into PBS solution (pH 7) without any lysozyme.

2.6. In Vitro Cytocompatibility Study. The finely grounded powder of c-Dxt/pAA 8 xerogel was filled in a stainless steel disk followed by placing a second steel disk on the top. The sandwich disks were transferred onto a pistil in a hydraulic press. Pressure was provided for a few seconds on the sandwiched disk containing the xerogel. The pressure was then released. The disks were pulled apart to retrieve the pellets. For pellet preparation, the equivalent weight of powder c-Dxt/pAA 8 xerogel was used. The pellets were put in 24-well plates for in vitro studies. The pellets were sterilized by 70% ethanol and UV after frequent washing with sterilized phosphate buffer solution (pH 7.4). After aspiration of PBS, pellets were incubated overnight for protein adsorption with α-MEM (Gibco) media supplemented with 10% FBS, 1% penicillin/streptomycin solution and 3.7% sodium bicarbonate at 37 °C in a 5% CO_2 atmosphere.[38] Media from the 24 well plates was then aspirated and the pellets were seeded with 2 × 10^5 human mesenchymal stem cells (hMSCs). The hMSCs were acquired from Advanced Neuro-Science Allies, Bangalore, India. Media were replaced after 24 h and every 48 h thereafter. Cells were also seeded on lysine coated slides. After 1, 3, and 7 days, cell morphology was assessed by rhodamine−phalloidin (catalog no. R415, Invitrogen) and DAPI (4′,6-diamidino-2-phenylindole, catalog no. D1306, Invitrogen) in accordance with the manufacturer's instructions. Briefly, the cells were fixed, permeabilized using Trition-X-100 followed by blocking the nonspecific sites using bovine serum albumin (Sigma). The cells were then stained with the florescent dyes and imaged using a florescence microscope (Zeiss Axio Observer Z1, Carl Zeiss, Germany). MTT [3-(4, 5-dimethylthiazol-2-yl)-2, 5-diphenyl tetrazolium bromide] assay was performed to examine the rate of cell proliferation on the pellets after 1, 3, and 7 days as reported earlier.[9,38] For repeatability, the test was performed in triplicate. All data in this study were expressed as the mean ± standard deviation. Statistical analysis was performed using one-way ANOVA followed by tukey post hoc analysis in Origin Pro 8 software. Significance was determined at $p < 0.05$.

2.7. Determination of Equilibrium Swelling Ratio (ESR), Deswelling Ratio (DSR) and Its Kinetics. The stimulus-responsive behavior of synthesized hydrogels was investigated by varying the pH and temperature of the media.

2.7.1. pH Responsive Behavior. The ESR of different c-Dxt/pAA hydrogels was determined at pH 1.2, 6.8, and 7.4 buffers at 37 °C.

2.7.2. Temperature Responsive Behavior. The swelling characteristics of different hydrogels were also studied at temperature of 32, 37 and 42 °C at a constant pH of 7.4.

To determine the reversible nature of the gel, deswelling characteristics was also performed using a known amount of fully swollen hydrogel at 37 °C with 100 mL of 7.4 PBS on a constant temperature oven. The detailed procedures for the measurement of ESR and DSR have been explained in the Supporting Information.

2.7.3. Swelling and Deswelling Kinetics. The swelling and deswelling rate of the hydrogel were determined using Voigt model (eq 1):[39,40]

$$S_t = S_e(1 - e^{-t/\tau}) \quad (1)$$

S_t ($g \cdot g^{-1}$) and S_e ($g \cdot g^{-1}$) demonstrate the swelling at time t and the equilibrium swelling, respectively; t stands for the time (min) for swelling and τ (min) stands for the rate parameter. The τ value represents the swelling/deswelling rate, that is, the lower the τ value, the higher the swelling/deswelling rate.[39,40]

2.8. In Vitro Ornidazole and Ciprofloxacin Release Studies. *2.8.1. Preparation of Tablets.* The ornidazole and ciprofloxacin tablets were prepared for in vitro release study using following

DOI: 10.1021/am508712e
ACS Appl. Mater. Interfaces 2015, 7, 4791−4803

Table 1. Details of Synthetic Parameters, % CR, and % ESR of Various Hydrogels[a]

hydrogels	initiator concn ($\times 10^{-6}$)	cross-linker concn ($\times 10^{-3}$)	monomer concn ($\times 10^{-1}$)	% CR	% ESR at 37 °C		
					pH 1.2	pH 6.8	pH 7.4
c-Dxt/pAA 1	1.85	3.23	1.50	65.03	86 ± 1	298 ± 12	1720 ± 86
c-Dxt/pAA 2	3.70	3.23	1.50	66.71	83 ± 2	289 ± 11	1510 ± 75
c-Dxt/pAA 3	9.25	3.23	1.50	75.50	80 ± 7	252 ± 10	1390 ± 69
c-Dxt/pAA 4	18.50	3.23	1.50	63.25	130 ± 13	515 ± 13	3401 ± 170
c-Dxt/pAA 5	9.25	4.86	1.50	79.85	75 ± 6	237 ± 10	1262 ± 63
c-Dxt/pAA 6	9.25	6.48	1.50	84.34	68 ± 7	203 ± 11	1201 ± 60
c-Dxt/pAA 7	9.25	8.10	1.50	64.65	106 ± 7	332 ± 14	1936 ± 96
c-Dxt/pAA 8	9.25	6.48	1.87	90.45	63 ± 8	195 ± 12	1154 ± 57
c-Dxt/pAA 9	9.25	6.48	2.25	64.89	89 ± 8	306 ± 12	1702 ± 85
c-Dxt/pAA 10	9.25	6.48	2.62	64.73	115 ± 9	446 ± 12	2620 ± 131

[a]For all hydrogel synthesis, the amount of dextrin is 6.2×10^{-3} moles (i.e., 1g).

composition: c-Dxt/pAA xerogel−drug−PVP (binder) = 450:500:50 mg. The detailed procedure for the preparation of tablet has been given in the Supporting Information.

2.8.2. Drug Release Study and Determination of % Erosion. Release Study at Various pH. The in vitro release of cumulative drugs (ornidazole/ciprofloxacin) from c-Dxt/pAA was executed using dissolution apparatus (Lab India, DS 8000) at 37 ± 0.5 °C. The rotation speed of the paddle was 60 rpm. The release study was performed using 900 mL of acidic buffer (pH 1.2) for 2 h, phosphate buffer having pH 6.8 for next 3 h (for the colonic drug ornidazole) followed by pH 7.4 buffer up to 18 h. The percent cumulative drug release was measured using UV−visible spectrophotometer (Shimadzu, Japan; UV 1800). The release kinetics and mechanisms were evaluated using various models. The details of different kinetics and mechanism models have been explained in the Supporting Information.

Release Study at Different Temperatures. To observe the effect of temperature on ornidazole/ciprofloxacin delivery from c-Dxt/pAA hydrogel, we also performed a release study at three different temperatures (i.e., 32, 37, and 42 °C) in a steady rotation of 60 rpm. The release kinetics and mechanisms were verified by fitting the release data to various models, details of which have been explained in the Supporting Information.

During drug release from hydrogel systems, erosion took place after attaining the critical gel concentration of the hydrogel. The % erosion was determined as stated in the Supporting Information.

2.8.3. Drug Stability Study. The stability of tablet formulations were performed up to 3 months as reported earlier,[9] principally to observe the effect of environmental factors on release characteristics. The detailed procedure has been provided in the Supporting Information.

3. RESULTS AND DISCUSSION

3.1. Synthesis of Cross-Linked Hydrogel. The poly(acrylic acid) chains were cross-linked onto dextrin in the presence of MBA cross-linker. It is believed that potassium persulfate creates free radical sites on dextrin backbone, which further reacts with AAc to propagate the chain reaction. Because of the presence of four reactive sites (due to the existence of two unsaturated double bonds on MBA),[41] MBA would be polymerized and cross-linked with the radicals generated on dextrin grafted with pAA network, as proposed in Scheme 1. This results in the formation of a 3-D cross-linked network. To investigate the effect of reaction parameters, we synthesized various hydrogels and selected the best grade (i.e., c-Dxt/pAA 8) with higher percent cross-linking (% CR) and lower % ESR (Table 1).

3.1.1. Effect of Reaction Parameters. For the development of hydrogel, the concentration of initiator was altered from 1.85 $\times 10^{-6}$ mol to 18.50 $\times 10^{-6}$ mol. It was observed that c-Dxt/pAA 8 demonstrates lower % ESR (i.e., higher % CR). This is because at relatively higher initiator concentration, the maximum number of free radical sites would generate on the dextrin backbone as well as on the grafted network, which would be cross-linked in the presence of MBA, resulting in higher % CR.

The cross-linker concentration was varied from 3.23 $\times 10^{-3}$ to 8.1 $\times 10^{-3}$ mol, keeping other parameters constant (Table 1). Maximum % CR (i.e., minimum % ESR) was obtained with the MBA concentration of 6.48 $\times 10^{-3}$ mol, due to the incorporation of maximum amount of cross-linker in the hydrogel structure. Consequently, a more rigid structure would form, which results in lower % ESR.

With the increase in acrylic acid concentration from 1.50 $\times 10^{-1}$ mol to 2.62 $\times 10^{-1}$ mol, it was found that the % ESR increased, signifying lower % CR (Table 1). This is probably because of more homopolymer formation with elevated monomer concentration.[9]

3.2. Characterization. The FTIR spectrum of dextrin[18] (Table S1, Supporting Information) reveals that the peaks at 3495 and 2940 cm^{-1} are responsible for O−H and C−H stretching vibrations. The peaks at 1092 and 1026 cm^{-1} are attributed to C−O−C stretching vibrations. The FTIR spectrum of acrylic acid demonstrates that the corresponding peaks at 3543 and 2968 cm^{-1} are assigned to O−H and C−H stretching vibrations, respectively. The peaks at 1726 and 1189 cm^{-1} are responsible for −COOH and C−O stretching vibrations. The peak at 1638 cm^{-1} is assigned to C═C stretching vibrations (Table S1, Supporting Information). Figure S1a, Supporting Information shows the FTIR spectrum of c-Dxt/pAA 8 xerogel. The O−H stretching frequency of the dextrin and the acrylic acid and N−H stretching frequency of MBA overlap and form a broad peak that appears at 3446 cm^{-1}. The two strong peaks at 1726 and 1169 cm^{-1} are characteristics to stretching frequencies of the carboxylic acid groups (i.e., C═O and C−O), suggesting that poly(acrylic acid) chains are present on dextrin moiety. The two peaks at 1620 and 1540 cm^{-1} are responsible for amide-I and amide-II stretching vibrations of MBA. The peak at 1403 cm^{-1} signifies the presence of C−N group, which further suggests the incorporation of cross-linker (i.e., MBA) in the hydrogel network. Besides, the absence of peak at 1638 cm^{-1} (which is for C═C, present in acrylic acid) in the hydrogel structure confirms the polymerization of acrylic acid. Various peaks corresponding to different functional groups of ornidazole and ciprofloxacin have been reported in Table S1 (Supporting Information). In the FTIR spectra of triturated form of

DOI: 10.1021/am508712e
ACS Appl. Mater. Interfaces 2015, 7, 4791−4803

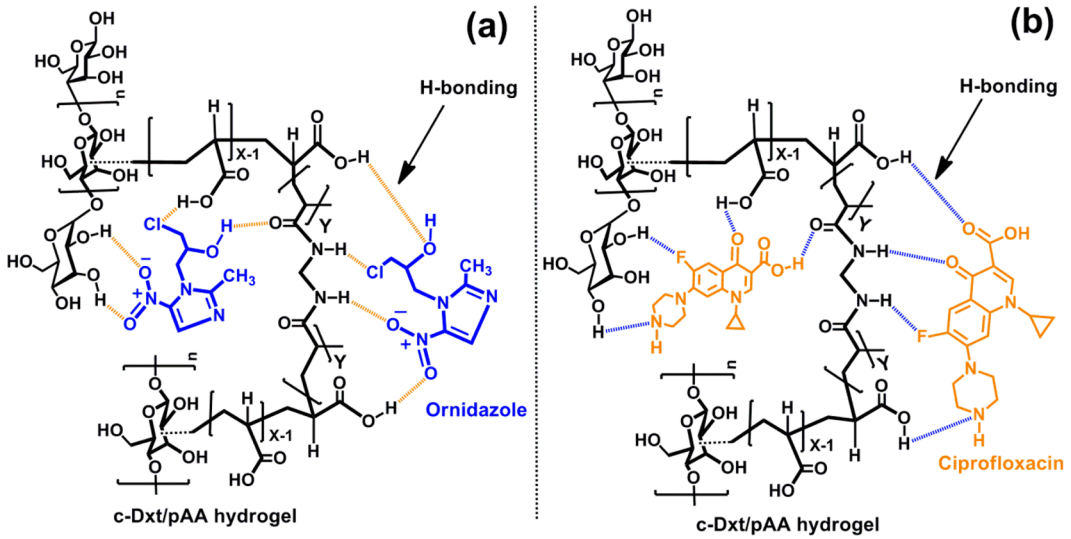

Figure 1. Probable interactions between c-Dxt/pAA hydrogel and (a) ornidazole and (b) ciprofloxacin drugs.

ornidazole and ciprofloxacin tablets (Figure S1b,c and Table S1, Supporting Information), the C═O stretching frequency of −COOH groups shifted from 1726 to 1711 cm^{-1} for ornidazole and to 1720 cm^{-1} for ciprofloxacin; −OH stretching frequency shifted from 3446 to 3418 cm^{-1} for ornidazole and to 3427 cm^{-1} for ciprofloxacin; amide-I (of MBA) from 1620 to 1610 cm^{-1} for ornidazole and to 1612 cm^{-1} for ciprofloxacin, amide-II (of MBA) stretching frequency shifted from 1540 to 1529 cm^{-1} for ornidazole and to 1520 cm^{-1} for ciprofloxacin. The shifting of these peaks signifies the probable H-bonding interactions between the hydrogel and the drugs in tablet formulations, as shown in Figure 1.

Figure 2 describes the UV−vis−NIR spectra of c-Dxt/pAA 8 xerogel, pure ornidazole, and ciprofloxacin drugs and their corresponding tablet formulations. It is obvious that the characteristic peaks of ornidazole and ciprofloxacin are attributed to the conjugation in imidazole ring and quinolones

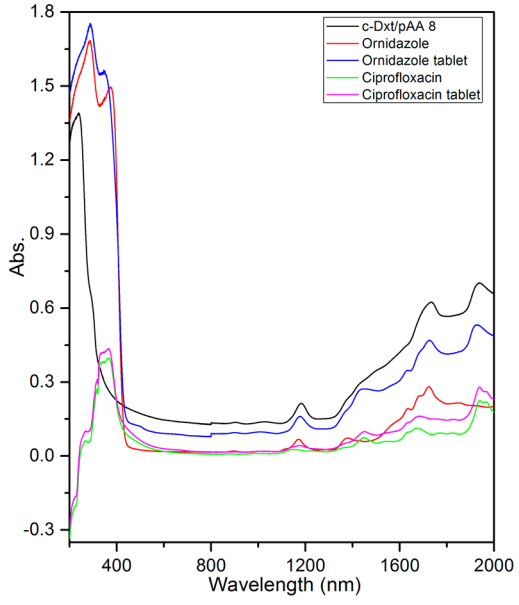

Figure 2. UV−vis−NIR spectra of c-Dxt/pAA 8 xerogel, ornidazole, ciprofloxacin, and triturated form of corresponding tablets.

ring, respectively. However, the tablet formulations showed blue shift (for ornidazole 371.6 → 346.1 and for ciprofloxacin 366.9 → 361.6 nm), which confirms the physical interactions between the drugs and the hydrogel, as proposed in Figure 1.

^{1}H NMR spectrum of dextrin (Figure S2, Supporting Information, DMSO-d_6, 400 MHz, ppm): the peaks between δ = 3.323 and 4.450 are attributed to protons at positions 2, 3, 4, 5, and 6 (H^2−H^6). While the peaks between δ = 4.962 and 5.061 are due to anomeric proton (H^1). The peaks between δ = 5.362 and 5.449 corresponds to the anomeric proton for α-1,6 linkages (<5% of the total dextrin).[32] Besides, peaks between δ = 2.996 and 3.042 and δ = 2.861 and 2.926 indicate the presence of protons for primary and secondary hydroxyl groups, respectively.

^{1}H NMR spectrum of acrylic acid (Figure S3, Supporting Information, DMSO-d_6, 400 MHz, ppm): δ = 12.416 (s, 1H; i.e., for H^1), 6.150−6.372 (m, 1H; i.e., for H^2), 6.014−6.094 (m, 1H; i.e., for H^4), and 5.838−5.954 (m, 1H; i.e., for H^3).

^{1}H NMR spectrum of MBA (Figure S4, Supporting Information, DMSO-d_6, 400 MHz, ppm): δ = 8.744 (m, 1H; i.e., for H^2), 6.226−6.358 (m, 1H; i.e., for H^3), 6.099−6.199 (m, 1H; i.e., for H^5) and 4.549−4.608 (m, 2H; i.e., for H^1).

The polymerization of monomers and the formation of chemically cross-linked network have been confirmed by monitoring the development and decomposition of chemical shifts of the NMR spectra of the reactants.[28] The deviation in the intensity of the characteristic chemical shifts with cross-linker concentration was used to determine the cross-linking density of the c-Dxt/pAA 8 hydrogel.[28]

Figure 3 demonstrates the ^{1}H NMR spectra (DMSO-d_6, 400 MHz, ppm) of reaction mixtures for the development of c-Dxt/pAA 8 hydrogel at different time intervals (only reactants and reaction mixture after 5, 15, and 20 min of MBA addition). The ^{1}H NMR signals for the protons of the c-Dxt/pAA 8 hydrogel have been symbolized as A for −CH− at the chemical shift ∂ = 1.672 and B for $-CH_2$ at ∂ = 1.310 owing to the existence of poly(acrylic acid) as well as MBA molecules, K for −NH at ∂ = 8.724, and D for methylene ($-CH_2-$) groups between two −NH groups of MBA at ∂ = 4.533.

The vinyl protons of the acrylic acid (AAc) and cross-linker (MBA) have been denoted as E at ∂ = 5.889, F at ∂ = 6.004, G at ∂ = 6.226, and carboxylic acid protons as I at ∂ = 12.271.

DOI: 10.1021/am508712e
ACS Appl. Mater. Interfaces 2015, 7, 4791−4803

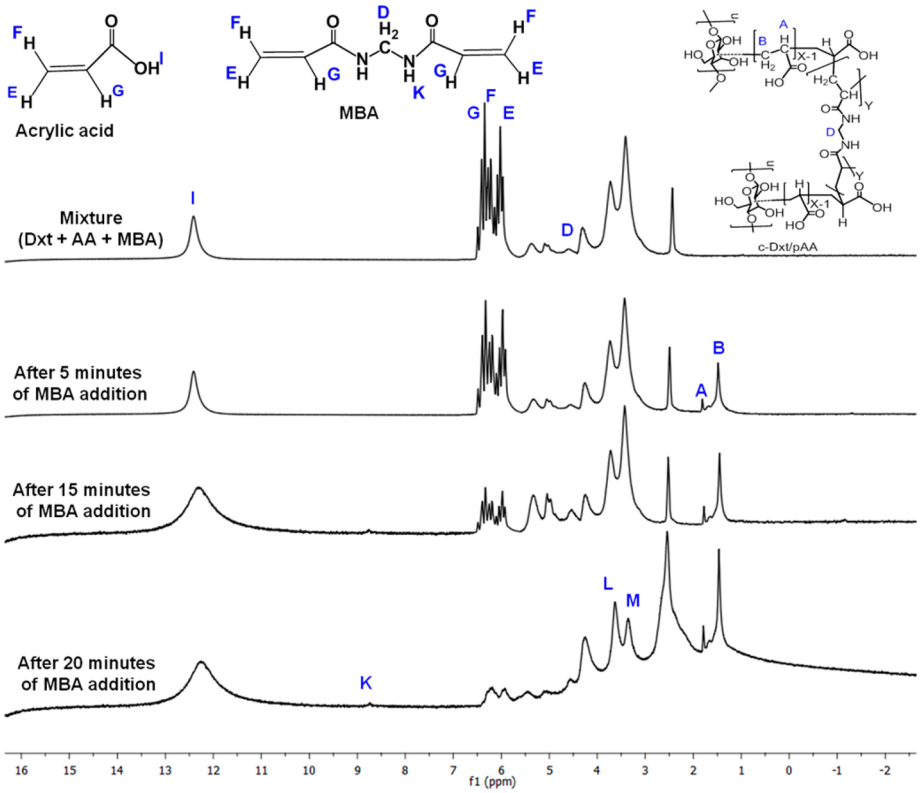

Figure 3. ^{1}H NMR spectra for the preparation of c-Dxt/pAA 8 hydrogel in DMSO-d_6.

Investigation of the NMR spectra suggested that the peaks at ∂ = 5.889−6.226 ppm in the mixture are owing to the vinyl protons E, F, and G of the acrylic acid and MBA. After 5 min of MBA addition, it was observed that the vinyl peaks (∂ = 5.889−6.226 ppm) gradually disappeared and the methylene peaks (∂ = 1.310−1.672 ppm) appeared, which imply the polymerization of acrylic acid. Again, the absence of peaks between δ = 2.861 and 3.042 indicate the reactivity of the hydroxyl groups of dextrin. Besides, with progress of time, the intensity of the methylene protons peak of cross-linker (H^D, at 4.533 ppm) gradually increased, which signify the incorporation of cross-linker (i.e., MBA) in the hydrogel network (Scheme 1).

Figure 4a shows the ^{1}H NMR spectrum of pure c-Dxt/pAA hydrogel after removal of homopolymer (DMSO-d_6, 400 MHz: δ = 12.271 (for H^I), 8.724 (for H^K), 5.398 (anomeric protons for α-1, 6 linkages of dextrin), 5.041 (for H^1), 4.553 (for H^D), 3.322−4.239 (for H^2−H^6), 2.520 (for DMSO), and 1.044−2.487 (for H^A and H^B). Thus, the absence of the vinylic protons (E, F, and G) in the hydrogel structure confirmed that both acrylic acid and MBA polymerized in the above reaction conditions, and the hydrogel is free from unreacted monomer and cross-linker. Again, the presence of peaks (H^D and H^K) also confirmed the successful occurrence of cross-linking reaction (Scheme 1).

3.2.1. Determination of Cross-Linking Density. The cross-linking density of c-Dxt/pAA 8 hydrogel was determined using the peak intensity of sp^3 carbon protons (i.e., H^A and H^B), which were formed from sp^2 carbon during the polymerization of acrylic acid and methylene protons of the cross-linker (i.e., H^D; see Figure 4a). The cross-linking density (CD) was measured using eq 2:[28]

$$\mathrm{CD} = \frac{\mathrm{Y}}{(\mathrm{X} + \mathrm{Y})} = \frac{I_\mathrm{D}}{I_\mathrm{B}} \qquad (2)$$

where X and Y represent the repeating units of acrylic acid and MBA in the synthesized hydrogel (Scheme 1). It is presumed that I_A and I_B (i.e., peak intensity of A and B, respectively) are directly proportional to the number of H^A and H^B protons and are comparative with (X + Y).[28] Besides, it is obvious that the ratio of peak area of A and B is more than half (A/B = 1:2.43, see Figure 4a). This replicates the fixed ratio between H^A and H^B in the network hydrogel.[28] Here, I_A has been assumed as 1, and with this hypothesis the intensity of peak D was calculated, which basically suggests the amount of MBA present in the hydrogel (i.e., cross-linking density).[28] Here, the CD of c-Dxt/pAA 8 hydrogel was found to be 52.26% (having I_A = 1, I_B = 2.43, and I_D = 1.27; Table 2)

The solid state ^{13}C NMR spectrum of the c-Dxt/pAA 8 xerogel is demonstrated in Figure 4b. The NMR spectrum of dextrin provides the characteristics peaks at δ = 111.4, 88.5, 79.4, and 68.1 ppm.[9] While the c-Dxt/pAA 8 xerogel shows some extra peaks. The peak at 176.1 ppm is associated with carbon atoms of carboxylic acid groups (Figure 4b). Peaks at 41.7 and 35.6 ppm are assigned to sp^3 hybridized carbon atoms, which were formed through the polymerization of the acrylic acid and cross-linker, as shown in Scheme 1 (i.e., during polymerization, two sp^2 hybridized carbon atoms of AAc monomer converted to sp^3 hybridized carbon atoms).

Thus, from the ^{1}H and ^{13}C NMR spectra, it is apparent that the poly(acrylic acid) chains have been cross-linked on dextrin in the presence of the MBA cross-linker.

Thermogravimetric analysis of dextrin reveals two distinct regions of weight loss (Figure 5). The initial decomposition is due to the presence of a minute quantity of moisture in the

DOI: 10.1021/am508712e
ACS Appl. Mater. Interfaces 2015, 7, 4791−4803

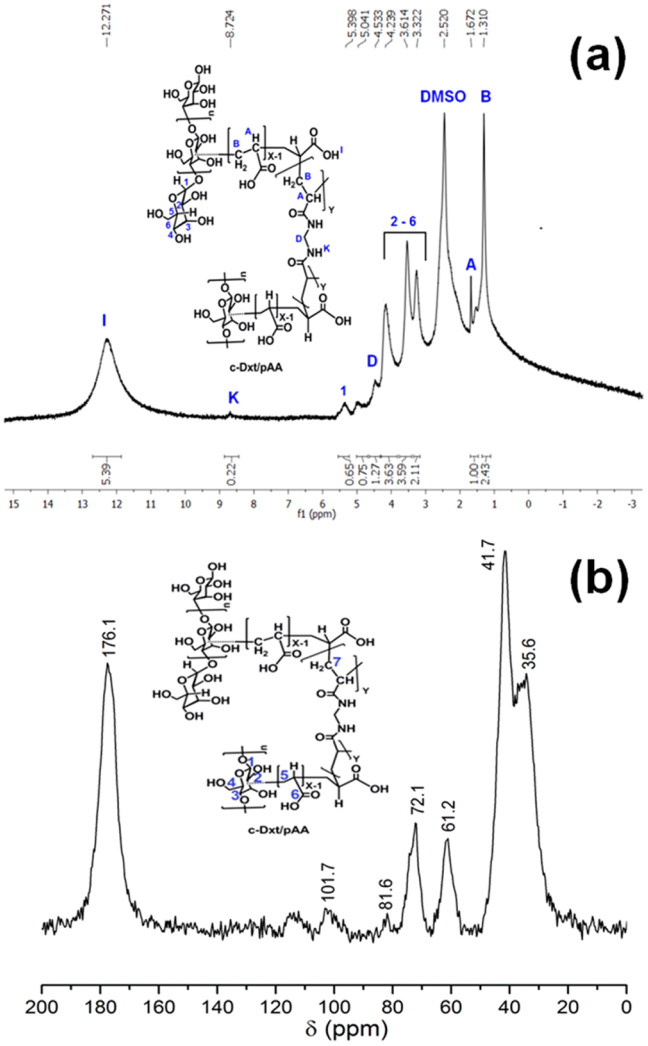

Figure 4. (a) ^{1}H NMR spectrum of c-Dxt/pAA 8 hydrogel in DMSO-d_6 and (b) solid state ^{13}C NMR spectrum of c-Dxt/pAA 8 xerogel.

Table 2. Peak Intensity and Crosslink Density of c-Dxt/pAA 8 Hydrogel

hydrogel	I_A	I_B	I_D	cross-linking density (%)
c-Dxt/pAA 8	1	2.43	1.27	52.26

biopolymer. The second zone of weight loss (i.e., 250−330 °C) is owing to the degradation of dextrin moiety. The thermogram of the c-Dxt/pAA 8 xerogel (Figure 5) demonstrates two supplementary weight loss regions, in the range of 105−180 and 325−460 °C, which are responsible for the decomposition of cross-linked MBA and the elimination of CO_2 from the hydrogel structure (from pAA), respectively. This confirms the successful incorporation of pAA chains on dextrin moiety in the presence of cross-linker.

The CHN analysis results are given in Table S2, Supporting Information. It is obvious that there is substantial increase in % O in the xerogel, suggesting the successful incorporation of poly(acrylic acid) chains. Besides, the increase in % N supports the presence of cross-linker in c-Dxt/pAA 8 xerogel.

The FESEM image of the dextrin (Figure 6a) reveals that it has granular morphology, while that of xerogel's (c-Dxt/pAA 8; Figure 6b) surface is porous in nature. The various interconnected pores after lyophilization of the c-Dxt/pAA 8

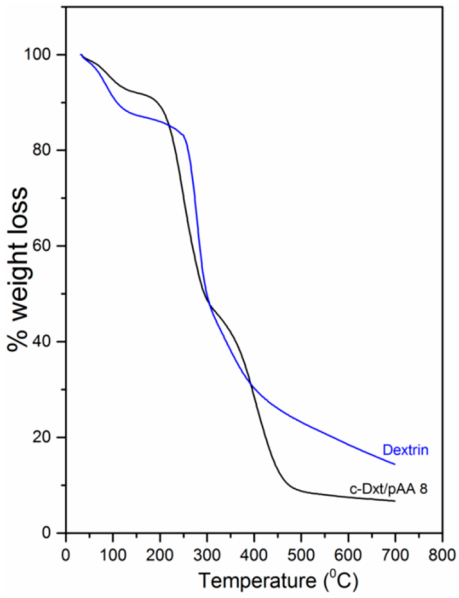

Figure 5. TGA curves of dextrin and c-Dxt/pAA 8 xerogel.

hydrogel network (in swollen state, aqueous media using pH 7.4 buffer) is evidenced in the E-SEM image (Figure 6c), which confirmed its porous morphology. The interconnection between pores could be attributed to the cross-linking network formation in the gels. It is assumed that these interconnected pores permit the easy flow of drugs into the hydrogel.

Rheological characteristics of dextrin and different hydrogels were investigated in PBS media, pH 7.4. Oscillatory sweep measurements were executed to evaluate the modulii of the dextrin solution (Figure S5, Supporting Information). It was observed that the viscous modulus (G'') of dextrin solution was higher than the elastic modulus (G'), indicating the sol state of the solution. After cross-linking reaction with acrylic acid in the presence of MBA, both modulii increased in c-Dxt/pAA 8 at 37 and 70 °C as evidenced from the frequency sweep experiments (Figure 7a and Figure S6a, Supporting Information). However, the higher value of G' than that of G'' suggests the gel state of c-Dxt/pAA 8 hydrogel. Moreover, the increase of G' and G'' with frequency at 37 and 70 °C (Figure 7a and Figure S6a, Supporting Information) indicate the elastic nature of the c-Dxt/pAA 8 hydrogel. In addition, the variation in shear viscosity with change in shear rate in the c-Dxt/pAA 8 hydrogel is provided in Figure S7, Supporting Information. The hydrogel exhibited non-Newtonian shear thinning flow behavior.

Gelation time was measured by dynamic time and dynamic frequency sweeps at various cure times using parallel plate geometry at the reaction temperature (i.e., at 70 °C). For this measurement, 1 Pa stress was applied at frequencies (ω) ranging from 0.5 to 3.0 Hz to minimize the trouble in the gelation process. It was reported before that the point at which loss tangent (tan δ) vs time curves joined at various frequencies is defined as the gel point.[34,42,43] From Figure 7b, it was observed that tan δ converge at ∼879 s, suggesting the gelation time of the c-Dxt/pAA 8 hydrogel. In addition, the gelation time was also determined from the time sweep experiments (Figure 7c). It is obvious that G', G'' intersect at ∼854 s, which confirmed the beginning of gelation process, and the time indicates the gelation time. The small difference in time (i.e., 879 and 854 s), which was observed from two different methods, can be explained on the basis of the differences

DOI: 10.1021/am508712e
ACS Appl. Mater. Interfaces 2015, 7, 4791−4803

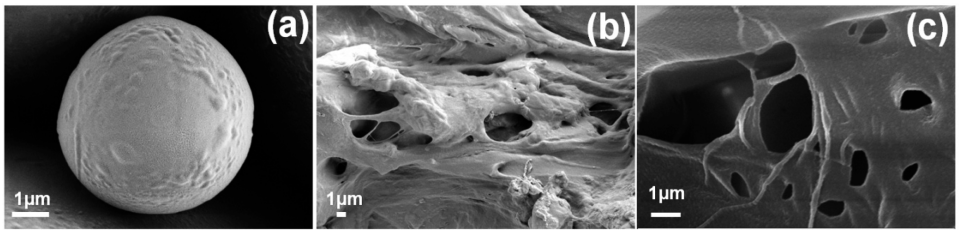

Figure 6. FESEM surface images of (a) dextrin and (b) c-Dxt/pAA 8 xerogel and (c) E-SEM surface image of c-Dxt/pAA 8 hydrogel at swollen state (aqueous media using pH 7.4 buffer).

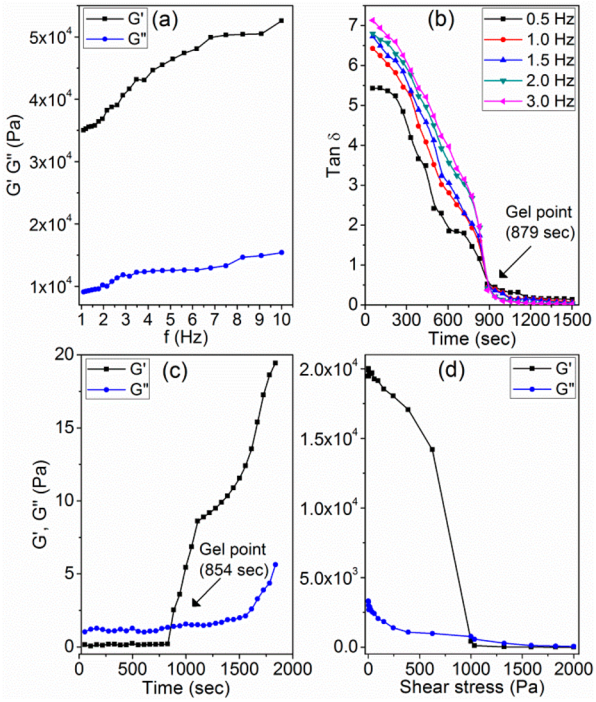

Figure 7. Plots of (a) G', G'' vs frequency (b) tan δ vs time, (c) G', G'' vs time and (d) G', G'' vs shear stress for c-Dxt/pAA 8 hydrogel.

between the applied strain and frequencies during the experiment.[34]

The stress zone beyond which G' is independent of applied shear stress is the linear viscoelastic region (LVR).[43] Beyond the LVR, both G', G'' abruptly decreased for all the hydrogels, indicating breakdown of the network structure (Figure 7d and Figure S8, Supporting Information).[33] This is because with increase in shear stress, the entanglements of polymer network distorted. This leads to the decrease in the modulus values. The critical stress value, where the cross-linked network collapsed, is known as yield stress (σ).[33] The yield stress values of various hydrogels are reported in Table 3, and it has been found that c-Dxt/pAA 8 has highest σ value, indicating a stronger gel network. When the temperature was increased from 37 to 70 °C, no significant difference was observed on the yield stress and gel strength of c-Dxt/pAA 8 hydrogel (Figure 7d and Figure S6b, Supporting Information). This suggests that the c-Dxt/pAA 8 hydrogel is thermally stable with sufficient gel strength at 37 and 70 °C.

3.3. In Vitro Cytocompatibity Study and Cell Proliferation. The cell viability and proliferation studies predict the cellular compatibility of a biomaterial intended for drug delivery applications.[9] The cellular attachment on pellet of c-Dxt/pAA 8 hydrogel and control (lysine coated slides) was

Table 3. Gel Strength of Various Hydrogels at 37 °C

hydrogels	yield stress (σ) (Pa)	G'/G''
c-Dxt/pAA 1	543	12.73
c-Dxt/pAA 2	554	12.83
c-Dxt/pAA 3	566	12.90
c-Dxt/pAA 4	501	11.86
c-Dxt/pAA 5	582	13.33
c-Dxt/pAA 6	601	13.66
c-Dxt/pAA 7	524	12.31
c-Dxt/pAA 8	624	14.35
c-Dxt/pAA 9	529	12.51
c-Dxt/pAA 10	511	12.10

assessed by rhodamine-phalloidin and DAPI assay at different time periods (Figure 8a). It is evident that the morphology of the cells cultured on control was similar to that of the cells grown on c-Dxt/pAA 8 hydrogel. On day 1, the cells were few in number, and the cytoskeleton was not well extended. On day 3, the cells on both the control and experimental grew bigger in size, while on day 7, the cells reached confluency and displayed extended actin filaments. This was further supported by MTT reduction assay (Figure 8b).

The c-Dxt/pAA 8 hydrogel and the tissue culture plate (TCP) sustained feasible population of mesenchymal stem cells right through the study period. The absorbance values obtained from MTT assay were converted to the rate of cell proliferation using standard curve (Figure 8b). After 7 days, the number of cells on c-Dxt/pAA 8 hydrogel and TCP were $5.8 \pm 0.66 \times 10^5$ and $5.1 \pm 0.60 \times 10^5$, respectively (at the 0.05 level, the population means are significantly different). The relatively higher number of cell population on c-Dxt/pAA 8 hydrogel may be because of the three-dimensional network of the hydrogel that facilitate more surface area for cells attachment and proliferation. The results indicate the cytocompatibility and nontoxic nature of c-Dxt/pAA 8.

3.4. Biodegradation Study. Figure S9 (Supporting Information) represents the biodegradation study result for c-Dxt/pAA 8 xerogel film after 0, 3, 7, 14, and 21 days. Hen egg white lysozyme have an analogous main chain formation and binding subsites as human lysozyme and PBS to stimulate in vivo conditions.[36] During the study, it was observed that the mass of the cross-linked hydrogel declined progressively. Lysozyme degrade the polysaccharides through enzymatic hydrolysis of the glycosidic bonds by the hexameric sugar ring binding sites of the lysozyme.[35,36] Once the number of suitable sites was reduced, the rate of degradation decreased between 7 and 21 days.

3.5. Swelling Characteristics of Hydrogel. *3.5.1. pH Responsive Swelling Behavior.* The swelling characteristics of dextrin and developed hydrogels were studied at different buffer media of pH 1.2, 6.8, and 7.4 at 37 °C (Figure 9 a–c and Table

DOI: 10.1021/am508712e
ACS Appl. Mater. Interfaces 2015, 7, 4791−4803

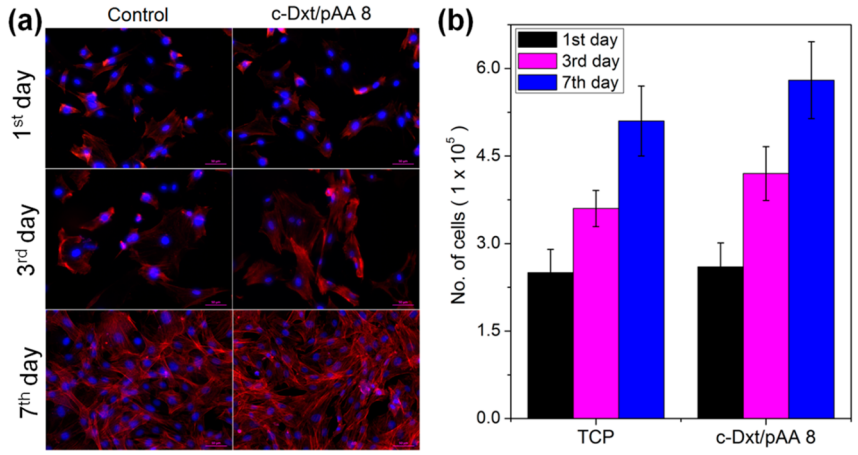

Figure 8. (a) Cellular attachment on pellet of c-Dxt/pAA 8 hydrogel and control (lysine coated slides) by rhodamine-phalloidin and DAPI assay at different time periods, (b) cell proliferation result of c-Dxt/pAA 8 hydrogel by MTT assay.

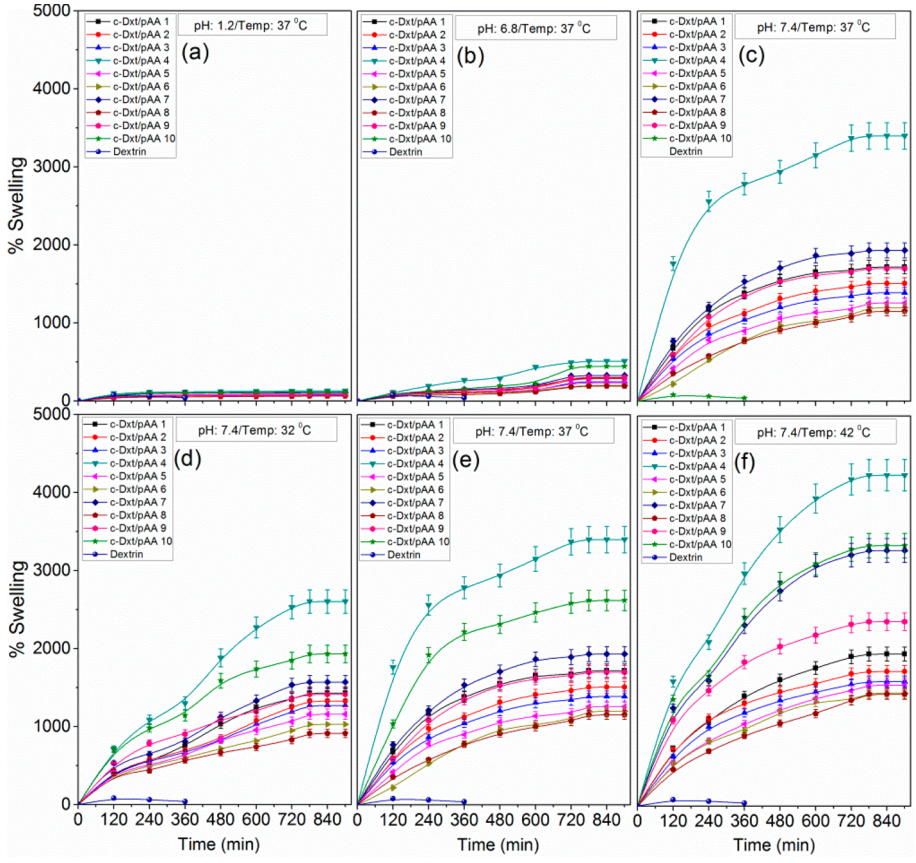

Figure 9. Swelling characteristics of dextrin and different hydrogels at (a) pH 1.2/37 °C, (b) pH 6.8/37 °C, (c) pH 7.4/37 °C, (d) pH 7.4/32 °C, (e) pH 7.4/37 °C, and (f) pH 7.4/42 °C. Results represented are mean ± SD, n = 3.

1). Dextrin demonstrated decreasing trend of swelling with time, signifying its solubility in aqueous media.[9] The equilibrium swelling of all the hydrogels was attained at ~13 h (Figure 9). It was also observed that the hydrogels exhibit higher % ESR than that of dextrin. This is due to the presence of pAA chains as well as cross-linker on the hydrogel structure, which enhanced the hydrophilicity of the network. This results in an increase in the surface area of the network (due to 3-D network) and aids the hydration and expansion of the gel structure. Besides, the porous surface of hydrogel improved the diffusion of water in the gel network.[9] Out of various hydrogels, c-Dxt/pAA 8 demonstrates lowest % ESR (Table 1 and Figure 9), owing to its higher % CR (Table 1). The hydrogel with higher % CR has a gel network that is more rigid and dense and would swell relatively less compared to that of the hydrogel with lower % CR.[9] It was also observed that % ESR in alkaline medium is much higher than that of acidic/neutral conditions (Figure 9). This is because in acidic condition (i.e., pH 1.2), the hydrophilic groups of hydrogel network were protonated, which prevent the formation of H-bonding with water,[9] resulting less % ESR.

DOI: 10.1021/am508712e
ACS Appl. Mater. Interfaces 2015, 7, 4791−4803

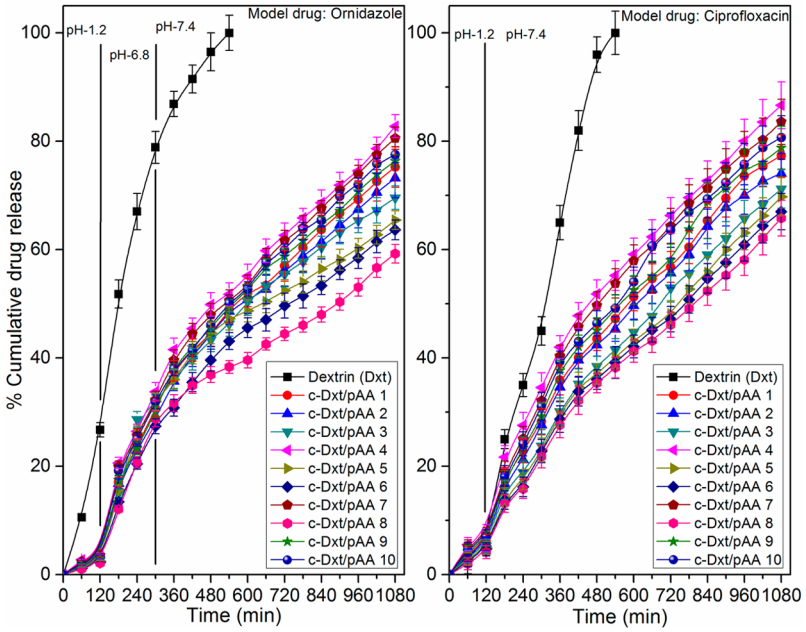

Figure 10. In vitro ornidazole and ciprofloxacin release profiles from c-Dxt/pAA hydrogels at different pH at 37 °C. The results represented here are mean ± SD (n = 3).

At pH 6.8, small number of −COOH groups of pAA may be deprotonated, which results in a slight increase in % ESR. However, in alkaline condition (pH 7.4), the maximum number of carboxylic acid groups would be deprotonated, which results in the formation of carboxylate ions ($-COO^-$). The COO^- groups would repeal each other, and thus, the gel network and the surface area would be expanded, resulting in higher % ESR.

3.5.2. Temperature-Responsive Swelling Behavior. The temperature-sensitive swelling characteristics of cross-linked hydrogels have shown in Figure 9d−f (the data are given in Table S3, Supporting Information). It is apparent that with increase in temperature, % ESR gradually enhanced. This is because at higher temperature, flexibility of the hydrogel network and diffusion of water molecules were increased. This facilitates the penetration of more water molecules into the hydrogel surface, resulting in higher % ESR at higher temperature as compared to lower temperature.

3.5.3. Swelling Kinetics. The rate of water absorption by hydrogel, that is, the diffusion rate of water into the hydrogel network under various physiological conditions (e.g., pH and temperature), has been determined using Voigt model.[39,40] At 37 °C and pH 7.4, the rate parameter values, τ (Table S4, Supporting Information) are lower than that of pH 1.2, which indicates that the diffusion rate of water molecules is higher in alkaline media compared to acidic media. This is mainly because of the formation of carboxylate ions in alkaline medium, which makes the polymer network more expanded. Among the various hydrogels, c-Dxt/pAA 8 has highest τ value because of its highest % cross-linking ratio. It was also observed that at 42 °C, the τ values (Table S4, Supporting Information) are lower than those at 32 and 37 °C, which signifies the higher swelling rate at higher temperature.

3.5.4. Deswelling Kinetics. Deswelling studies of c-Dxt/pAA hydrogels were investigated at different temperatures (32, 37, and 42 °C; Figure S10, Supporting Information). It is obvious that gel attains deswelling equilibrium at ∼13 h, after which it was in plateau. This behavior confirms the reversible nature of the hydrogel. The deswelling rate of hydrogel was also determined by measuring the rate parameter (τ) using Voigt model (Table S4, Supporting Information). It is obvious that τ values at 42 °C are lower, suggesting the higher deswelling rate at 42 °C than that at 37 and 32 °C.

3.6. In Vitro Ornidazole and Ciprofloxacin Release Studies. *3.6.1. pH-Sensitive Release Study.* Figure 10 represents the cumulative % of drugs release (ornidazole and ciprofloxacin) as a function of time. The release rate of a drug usually depends on the chemical structure, as well as on the % ESR of hydrogels.[44] The release of water-soluble drugs from tablet formulation using a hydrogel-based matrix occurs through the following steps: Initially, the drug molecules present on the surface of the hydrogel are released by the dissolution process, after which most of the drugs are released by the diffusion process, which was controlled by the penetration of the water molecules inside the gel network. Finally, minute amounts of drugs were released through erosion of the matrix.[9] It is evident (Figure 10) that release rate of ornidazole was higher at pH 6.8 and 7.4 than that of at pH 1.2. This may be because of the collapsed state of the hydrogel in acidic media owing to lower swelling rate.[9] Thus, the drug was incapable of disseminate from the hydrogels into the media.[9] Conversely, in alkaline pH, the hydrogels swelled fast, leading to an increase in drug diffusion from the matrix.[9] The same trend was also observed for ciprofloxacin release. Out of various synthesized hydrogels, c-Dxt/pAA 8 showed more sustained release behavior (∼59.25% ornidazole and ∼65.82% ciprofloxacin were released after 18 h). Moreover it was noticed that because of the cross-linked network, the % erosion of hydrogels are significantly lower than that of dextrin (Table S5, Supporting Information), which also supports the controlled release behavior of ornidazole and ciprofloxacin using c-Dxt/pAA hydrogels. The release study thus signifies that due to the chemical modification of dextrin using pAA and MBA, the hydrophilicity of the hydrogel network enhanced, which controlled the swelling behavior as well as minimized the % erosion. This results the release of enclosed drugs in more controlled way.

DOI: 10.1021/am508712e
ACS Appl. Mater. Interfaces 2015, 7, 4791−4803

Table 4. Values of Diffusion Coefficients for Ornidazole and Ciprofloxacin Release at Various pH and Temperatures[a]

	diffusion coefficients (cm^2/min)					
	ornidazole release at 6.8 buffer		ornidazole release at 7.4 buffer		ciprofloxacin release at 7.4 buffer	
hydrogels	D_i ($\times 10^{-5}$)	D_L ($\times 10^{-5}$)	D_i ($\times 10^{-5}$)	D_L ($\times 10^{-5}$)	D_i ($\times 10^{-5}$)	D_L ($\times 10^{-5}$)
c-Dxt/pAA 8 (32 °C)	12.11 ± 2.45	10.18 ± 0.95	4.31 ± 0.39	3.29 ± 0.63	7.12 ± 0.68	4.51 ± 0.51
c-Dxt/pAA 8 (37 °C)	9.04 ± 1.45	6.11 ± 0.45	3.39 ± 0.34	2.21 ± 0.55	6.75 ± 0.88	3.41 ± 0.31
c-Dxt/pAA 8 (42 °C)	7.52 ± 1.24	6.91 ± 0.77	3.02 ± 0.31	2.01 ± 0.52	5.36 ± 0.58	3.08 ± 0.47

[a]Tablet thickness = 0.70 (±0.01) cm.

3.6.2. Temperature-Sensitive Release Study. Figure S11 (Supporting Information) represents the cumulative percent of drugs release from c-Dxt/pAA 8 hydrogel as a function of time with variation of temperature. From the release profile (Figure S11, Supporting Information), it is evident that drug release is not remarkably affected by the variation of temperatures as that of pH. It was explained before that drug molecules remain in the hydrogel matrix by physical interaction (which was confirmed from FTIR and UV−vis−NIR analyses). For hydrogel systems, maximum amounts of drugs are released mainly through diffusion process.[4,5] Over time, water molecules diffuse into the hydrogel matrix, which results swelling of the gel. Simultaneously, drug molecules also diffuse from hydrogel to release media.

3.6.3. Drug Release Kinetics. Ornidazole and ciprofloxacin release kinetics from hydrogels were analyzed using zero order and first order kinetic models (details of kinetics models have been explained in Supporting Information). From various data given in Tables S6 and S7 (Supporting Information), it is evident that both ornidazole and ciprofloxacin release follow a first-order kinetics model more willingly than a zero-order kinetics model on the basis of higher R^2 value (Tables S6 and S7, Supporting Information).

3.6.4. Mechanism of Drug Release. Swelling characteristics can change the dimension and physicochemical properties of the hydrogel, which supports the drug release from hydrogel matrix.[9] The controlled release process follows the subsequent steps: (1) hydration, which took place due to the diffusion of the dissolution media into the tablet matrix;[9,45] (2) relaxation/erosion of the matrix; and (3) transport of the dissolved drug,[9,45] either through the hydrated matrix by diffusion process or from the eroded tablet to dissolution media.[45,46] Drug release from the hydrogel matrix usually occurs through either Fickian, non-Fickian, or Case II diffusion,[47,48] which is entirely dependent on the mechanical strength of the hydrogel, external stimulus, and chemical properties of the gel. To investigate the mechanism of the drug release, we used various linear and nonlinear mathematical models.

Among different mathematical models, the Korsmeyer−Peppas model[49] (for details, see the Supporting Information) provides the basic idea for the mechanism of drug release from hydrogel matrix. The Higuchi,[50] Hixson−Crowell,[51] and nonlinear Kopcha models[52] (see Supporting Information) elucidate the mechanism completely. For ornidazole and ciprofloxacin release, the n values (Tables S6 and S7, Supporting Information) were found to be between 0.45 and 0.89, suggesting that non-Fickian diffusion predominates for the release of both drugs from c-Dxt/pAA hydrogels.[9,47,48] This further signifies that both ornidazole and ciprofloxacin release depend on a combination of diffusion and erosion of the matrix. The R^2 values (Tables S6 and S7, Supporting Information) suggest that the release pattern follow the Higuchi model rather than the Hixson−Crowell model, which supports that diffusion process is responsible for drug release. In addition, the nonlinear Kopcha model measures quantitative contribution of diffusion and erosion process for drug release. In the case of ornidazole release, the exponent values (i.e., A and B; Tables S6−S7, Supporting Information) indicate that at pH 6.8 a major percentage of drugs are released by diffusion process while % erosion has a minute contribution. However, at pH 7.4, the release pattern showed that not only diffusion but also erosion is responsible for the controlled release behavior of ornidazole. On the contrary, for ciprofloxacin, the diffusion (A) and erosion exponent (B) values (Tables S6−S7, Supporting Information) specify that both diffusion and erosion are responsible for the sustained release characteristics.

3.6.5. Diffusion Coefficients Determination. The diffusion phenomenon occurs in the cylindrical shaped hydrogels during drug release and can be explained by Fick's first and second laws of diffusion using eqs 3 and 4, respectively.[41,48,53]

$$\frac{M_t}{M_\infty} = 4\left(\frac{D_i t}{\pi l^2}\right)^{1/2} \tag{3}$$

(M_t/M_∞) represents the fraction of drug release at time t, l is the thickness of the tablet, and D_i is the initial diffusion coefficient which was calculated from the slope of the plot between (M_t/M_∞) vs $t^{1/2}$.

The late diffusion coefficient (D_L) was calculated using eq 4 from the slope of the plot between ln $(1 - M_t/M_\infty)$ and t.[48,53]

$$\frac{M_t}{M_\infty} = 1 - \left(\frac{8}{\pi^2}\right)\exp\left[\frac{(-\pi^2 D_L t)}{l^2}\right] \tag{4}$$

From the calculated coefficient data for both ornidazole and ciprofloxacin in all media (Table S8, Supporting Information), it is apparent that D_i values are higher than D_L values. This suggests that the diffusion of ornidazole/ciprofloxacin drugs at the initial release state is faster than that at later stages. It has also been noticed that the values D_i and D_L for c-Dxt/pAA 8 hydrogel is lowest out of various hydrogels, which is attributed to its maximum % CR.

It was observed from Table 4 that with increasing temperature from 32 to 42 °C, the diffusion coefficient values decreased for both drugs. This suggests that the diffusion of drug molecules from c-Dxt/pAA 8 hydrogel is faster at higher temperature than at lower temperature. At lower temperature (i.e., 32 °C), the diffusion of water molecules in the hydrogel is lower, which makes the release rate slower. Whereas, at higher temperatures (i.e., 37 and 42 °C), water molecules will acquire more enthalpy, and consequently, the randomness of drug molecules increases. This results in the increase in diffusion of drug molecules at higher temperatures than that of lower temperatures. Moreover, a higher swelling rate at higher temperature also affects the release pattern. These combined

DOI: 10.1021/am508712e
ACS Appl. Mater. Interfaces 2015, 7, 4791−4803

effects are mainly responsible for the variation of drug release patterns at different temperatures.

3.6.6. Stability Study. The stability of ornidazole/ciprofloxacin tablets were performed under the influence of various environmental factors for 3 months. It is clear (from Table S1, FTIR analysis; Figure S12, XRD analyses; Figure S13 and Table S9, release characteristics, initially and after 3 months; Supporting Information) that the stability of ornidazole and ciprofloxacin using c-Dxt/pAA 8 hydrogel as carrier was ∼97 and ∼98%, respectively, up to 3 months.

4. CONCLUSIONS

From experimental observations and discussions, it is evident that various grades of novel, stimuli-responsive, biodegradable, nontoxic, chemically cross-linked, and porous hydrogels were developed based on dextrin, poly(acrylic acid), and MBA. Different physical and chemical characterizations confirmed the formation of a cross-linked network. The swelling and deswelling characteristics implied the reversible nature of the hydrogel. Cell proliferation study signifies that the hydrogel is noncytotoxic toward human mesenchymal stem cells (hMSCs). Biodegradation study using hen egg lysozyme confirmed the biodegradability of the hydrogel. Rheological studies confirmed the gelling behavior of c-Dxt/pAA hydrogel. The in vitro release and stability studies suggested that c-Dxt/pAA released the two different types of drugs (ornidazole and ciprofloxacin) in a sustained way with considerable stability up to 3 months. Thus, the above features of the c-Dxt/pAA hydrogel open a new platform as matrix for controlled release of ornidazole and ciprofloxacin.

■ ASSOCIATED CONTENT

Supporting Information

Details of swelling and deswelling study; details of tablet preparation method; various drug release kinetics and mechanism models; percent erosion; details of stability study method; FTIR spectra and data; ^{1}H NMR spectra of dextrin, acrylic acid, MBA; CHN analysis result; rheological characteristics of dextrin and hydrogels; biodegradation study; temperature responsive swelling data; swelling and deswelling kinetics parameters; deswelling characteristics of hydrogels; percent erosion results; in vitro drug release profiles at different temperatures; data of drug release kinetics and mechanism parameters at different pH; data of drug release kinetics and mechanism parameters at various temperatures; diffusion coefficient data at different pH values; XRD analysis result for stability test; drug release profile for stability study. This material is available free of charge via the Internet at http://pubs.acs.org.

■ AUTHOR INFORMATION

Corresponding Author

*Tel: +91-326-2235769. Fax: 0091-326-2296615. E-mail: sagarpal1@hotmail.com, pal.s.ac@ismdhanbad.ac.in.

Notes

The authors declare no competing financial interest.

■ ACKNOWLEDGMENTS

D.D. earnestly acknowledge University Grant Commission, New Delhi, India (ref. No.19-06/2011(i) EU-IV; Sr. No. 2061110303, Dated: 30.11.2011) for providing financial assistance Under Junior Research Fellowship Scheme. S.P. acknowledges the kind help of Dr. Animesh Ghosh, BIT, Mesra, India for the drug stability study and Department of Science and Technology, New Delhi, in form of a research grant (No.: SR/FT/CS-094/2009) to carry out the reported investigation.

■ REFERENCES

(1) Numata, P.; Yamazaki, S.; Naga, N. Biocompatible and Biodegradable Dual-Drug Release System Based on Silk Hydrogel Containing Silk Nanoparticles. *Biomacromolecules* **2012**, *13*, 1383−1389.

(2) Wei, J.; Chen, F.; Shin, J. W.; Hong, H.; Dai, C.; Su, J.; Liu, C. Preparation and Characterization of Bioactive Mesoporous Wollastonite−Polycaprolactone Composite Scaffold. *Biomaterials* **2009**, *30*, 1080−1088.

(3) Richardson, T. P.; Peters, M. C.; Ennett, A. B.; Mooney, D. J. Polymeric System for Dual Growth Factor Delivery. *Nat. Biotechnol.* **2001**, *19*, 1029−1034.

(4) Sylman, J. L.; Neeves, K. B. An Inquiry-Based Investigation of Controlled-Release Drug Delivery from Hydrogels: An Experiment for High School Chemistry and Biology. *J. Chem. Educ.* **2013**, *90*, 918−921.

(5) Saltzman, W. M.; Radomsky, M. L. Drugs Released from Polymers: Diffusion and Elimination in Brain Tissue. *Chem. Eng. Sci.* **1991**, *46*, 2429−2444.

(6) Ninawe, P. R.; Parulekar, S. J. Drug Delivery Using Stimuli-Responsive Polymer Gel Spheres. *Ind. Eng. Chem. Res.* **2012**, *51*, 1741−1755.

(7) Nita, L. E.; Nistor, M. T.; Chiriac, A. P.; Neamtu, I. Cross-Linking Structural Effect of Hydrogel Based on 2-Hydroxyethyl Methacrylate. *Ind. Eng. Chem. Res.* **2012**, *51*, 7769−7776.

(8) Chen, L.; Tian, Z.; Du, Y. Synthesis and pH Sensitivity of Carboxymethyl Chitosan-based Polyampholyte Hydrogels for Protein Carrier Matrices. *Biomaterials* **2004**, *25*, 3725−3732.

(9) Das, D.; Das, R.; Ghosh, P.; Dhara, S.; Panda, A. B.; Pal, S. Dextrin Crosslinked with Poly(HEMA): a Novel Hydrogel for Colon Specific Delivery of Ornidazole. *RSC Adv.* **2013**, *3*, 25340−25350.

(10) Jeong, J. H.; Schmidt, J. J.; Cha, C.; Kong, H. Tuning Responsiveness and Structural Integrity of a pH Responsive Hydrogel using a Poly(ethylene glycol) Cross-linker. *Soft Matter* **2010**, *6*, 3930−3938.

(11) Huynh, D. P.; Im, G. J.; Chae, S. Y.; Lee, K. C.; Lee, D. S. Controlled Release of Insulin from pH/Temperature-Sensitive Injectable Pentablock Copolymer Hydrogel. *J. Controlled Release* **2009**, *137*, 20−24.

(12) Im, J. S.; Bai, B. C.; In, S. J.; Lee, Y. S. Improved Photodegradation Properties and Kinetic Models of a Solar-Light-Responsive Photocatalyst When Incorporated into Electrospun Hydrogel Fibers. *J. Colloid Interface Sci.* **2010**, *346*, 216−221.

(13) Jin, S.; Gu, J.; Shi, Y.; Shao, K.; Yu, X.; Yue, G. Preparation and Electrical Sensitive Behavior of Poly(*N*-vinylpyrrolidone-co-acrylic acid) Hydrogel with Flexible Chain Nature. *Eur. Polym. J.* **2013**, *49*, 1871−1880.

(14) Meenach, S. A.; Hilt, J. Z.; Anderson, K. W. Poly(ethylene glycol)-based Magnetic Hydrogel Nanocomposites for Hyperthermia Cancer Therapy. *Acta Biomater.* **2010**, *6*, 1039−1046.

(15) Patil, N.; Roy, S. G.; Haldar, U.; De, P. CdS Quantum Dots Doped Tuning of Deswelling Kinetics of Thermoresponsive Hydrogels Based on Poly(2-(2-methoxyethoxy)ethyl methacrylate). *J. Phys. Chem. B* **2013**, *117*, 16292−16302.

(16) Wang, J.; Loh, K. P.; Wang, Z.; Yan, Y.; Zhong, Y.; Xu, Q. H.; Ho, P. C. Fluorescent Nanogel of Arsenic Sulfide Nanoclusters. *Angew. Chem., Int. Ed.* **2009**, *48*, 6282−6285.

(17) Taylor-Pashow, T. M. L.; Rocca, J. D.; Huxford, R. C.; Lin, W. Hybrid Nanomaterials for Biomedical Applications. *Chem. Commun.* **2010**, *46*, 5832−5849.

DOI: 10.1021/am508712e
ACS Appl. Mater. Interfaces 2015, 7, 4791−4803

(18) Das, D.; Das, R.; Mondal, J.; Ghosh, A.; Pal, S. Dextrin Crosslinked with Poly(lactic acid): A Novel Hydrogel for Controlled Drug Release Application. *J. Appl. Polym. Sci.* **2014**, *131*, 40039.
(19) Faraji, A. H.; Cui, J. J.; Guy, Y.; Li, L.; Gavigan, C. A.; Strein, T. G.; Weber, S. G. Synthesis and Characterization of a Hydrogel with Controllable Electroosmosis: A Potential Brain Tissue Surrogate for Electrokinetic Transport. *Langmuir* **2011**, *27*, 13635−13642.
(20) Albrecht, D. R.; Tsang, V. L.; Sah, R. L.; Bhatia, S. N. Photo-and Electropatterning of Hydrogel-Encapsulated Living Cell Arrays. *Lab Chip* **2005**, *5*, 111−118.
(21) Wu, D. Q.; Wu, J.; Chu, C. C. A Novel Family of Biodegradable Hybrid Hydrogels from Arginine-based Poly(ester amide) and Hyaluronic acid Precursors. *Soft Matter* **2013**, *9*, 3965−3975.
(22) Nakayama, Y.; Kim, J. Y.; Nishi, S.; Ueno, H.; Matsuda, T. Development of High-Performance Stent: Gelatinous Photogel-coated Stent that Permits Drug Delivery and Gene Transfer. *J. Biomed. Mater. Res.* **2001**, *57*, 559−566.
(23) Das, D.; Pal, S. Dextrin/poly (HEMA): pH Responsive Porous Hydrogel for Controlled Release of Ciprofloxacin. *Int. J. Biol. Macromol.* **2015**, *72*, 171−178.
(24) Lin, S.; Cao, C.; Wang, Q.; Gonzalez, M.; Dolbow, J. E.; Zhao, X. Design of Stiff, Tough, and Stretchy Hydrogel Composites via Nanoscale Hybrid Crosslinking and Macroscale Fiber Reinforcement. *Soft Matter* **2014**, *10*, 7519−7527.
(25) Elisseeff, J.; McIntosh, W.; Anseth, K.; Riley, S.; Ragan, P.; Langer, R. Photoencapsulation of Chondrocytes in Poly(ethylene oxide)-based Semi-interpenetrating Networks. *J. Biomed. Mater. Res.* **2000**, *51*, 164−171.
(26) Popescu, M. T.; Mourtas, S.; Pampalakis, G.; Antimisiaris, S. G.; Tsitsilianis, C. pH-Responsive Hydrogel/Liposome Soft Nanocomposites For Tuning Drug Release. *Biomacromolecules* **2011**, *12*, 3023−3030.
(27) Ding, C.; Zhao, L.; Liu, F.; Cheng, J.; Gu, J.; Dan, S.; Liu, C.; Qu, X.; Yang, Z. Dually Responsive Injectable Hydrogel Prepared by In Situ Cross-Linking of Glycol Chitosan and Benzaldehyde-Capped PEO-PPO-PEO. *Biomacromolecules* **2010**, *11*, 1043−1051.
(28) Arunbabu, D.; Shahsavan, H.; Zhang, W.; Zhao, B. Poly(AAc-*co*-MBA) Hydrogel Films: Adhesive and Mechanical Properties in Aqueous Medium. *J. Phys. Chem. B* **2013**, *117*, 441−449.
(29) Chiu, H. C.; Lin, Y. F.; Hsu, Y. H. Effects of Acrylic Acid on Preparation and Swelling Properties of pH-Sensitive Dextran Hydrogels. *Biomaterials* **2002**, *23*, 1103−1112.
(30) Abo-Shosha, M. H.; Ibrahim, N. A.; Allam, E.; El-Zairy, M. R.; El-Zairy, E. M. Synthesis and Characterization of Polyacrylic Acid/Dexy 85 and Polyacrylic Acid/Gum Arabic Adducts. *J. Appl. Polym. Sci.* **2006**, *101*, 4290−4300.
(31) Ding, X.; Li, L.; Liu, P. S.; Zhang, J.; Zhou, N. L.; Lu, S.; Wei, S. H.; Shen, J. The Preparation and Properties of Dextrin-Graft-Acrylic Acid/Montmorillonite Superabsorbent Nanocomposite. *Polym. Compos.* **2009**, *30*, 976−981.
(32) Molinos, M.; Carvalho, V.; Silva, D. M.; Gama, F. M. Development of a Hybrid Dextrin Hydrogel Encapsulating Dextrin Nanogel As Protein Delivery System. *Biomacromolecules* **2012**, *13*, 517−527.
(33) Pal, A.; Dey, J. K. Water-Induced Physical Gelation of Organic Solvents by *N*-(*n*-Alkylcarbamoyl)-L-alanine Amphiphiles. *Langmuir* **2011**, *27*, 3401−3408.
(34) Gibson, S. L.; Walls, H. J.; Kennedy, S. B.; Welsh, E. R. Reaction Kinetics and Gel Properties of Blocked Diisocyinate Crosslinked Chitosan Hydrogels. *Carbohydr. Polym.* **2003**, *54*, 193−199.
(35) Freier, T.; Koh, H. S.; Kazazian, K.; Shoichet, M. S. Controlling Cell Adhesion and Degradation of Chitosan Films by N-Acetylation. *Biomaterials* **2005**, *26*, 5872−5878.
(36) Justin, R.; Chen, B. Characterization and Drug Release Performance of Biodegradable Chitosan−Graphene Oxide Nanocomposites. *Carbohydr. Polym.* **2014**, *103*, 70−80.
(37) Masuda, T.; Ueno, Y.; Kitabatake, N. Sweetness and Enzymatic Activity of Lysozyme. *J. Agric. Food Chem.* **2001**, *49*, 4937−4941.
(38) Ghosh, P.; Rameshbabu, A. P.; Dogra, N.; Dhara, S. 2,5-Dimethoxy 2,5-Dihydrofuran Crosslinked Chitosan Fibers Enhance Bone Regeneration in Rabbit Femur Defects. *RSC Adv.* **2014**, *4*, 19516−19524.
(39) Rana, V.; Rai, P.; Tiwari, A. K.; Singh, R. S.; Kennedy, J. F.; Knill, C. J. Modified Gums: Approaches and Applications in Drug Delivery. *Carbohydr. Polym.* **2011**, *83*, 1031−1047.
(40) Omidian, H.; Hashemi, S. A.; Sammes, P. G.; Meldrum, I. Studies on Dynamic Mechanical and Mechanical Properties of Vinyloxyaminosilane Grafted Ethylene Propylene Diene Terpolymer/Linear Low Density Polyethylene (EPDM-g-VOS/LLDPE) Blends. *Polymer* **1998**, *39*, 816−823.
(41) Singh, B.; Sharma, N.; Chauhan, N. Synthesis, Characterization, and Swelling Studies of pH-Responsive Psyllium and Methacrylamide Based Hydrogels for the Use in Colon Specific Drug Delivery. *Carbohydr. Polym.* **2007**, *69*, 631−643.
(42) Henning, W. H.; Paul, M.; Francois, C. Stoichiometry Effects on Rheology of Model Polyurethanes at the Gel Point. *Macromolecules* **1998**, *21*, 532−535.
(43) Moura, M.; Jose, M.; Figueiredo, M.; Gil, M. H. Rheological Study of Genepin Cross-Linked Chitosan Hydrogels. *Biomacromolecules* **2007**, *8*, 3823−3829.
(44) Bardajee, G. R.; Pourjavadi, A.; Soleyman, R. Trigonal Pyramidal $CuInSe_2$ Nanocryastals Derived by a New Method for Photovoltaic Applications. *Colloids Surf., A* **2011**, *392*, 16−24.
(45) Das, R.; Pal, S. Hydroxypropyl Methyl Cellulose Grafted with Polyacrylamide: Application in Controlled Release of 5-Amino Salicylic Acid. *Colloids Surf., B* **2013**, *110*, 236−241.
(46) Kiortsis, S.; Kachrimanis, K.; Broussali, T.; Malamataris, S. Drug Release From Tableted Wet Granulations Comprising Cellulosic (HPMC or HPC) and Hydrophobic Component. *Eur. J. Pharm. Biopharm.* **2005**, *59*, 73−83.
(47) Peppas, N. A. Analysis of Fickian and Non-Fickian Drug Release from Polymers. *Pharm. Acta Helv.* **1985**, *60*, 110−111.
(48) Ritger, P. L.; Peppas, N. A. A Simple Equation for Description of Solute Release. I. Fickian and Non-Fickian Release from Non-Swellable Devices in the Form of Slabs, Spheres, Cylinders, or Discs. *J. Controlled Release* **1987**, *5*, 23−36.
(49) Korsemeyer, R. W.; Gurny, R.; Doelker, E.; Buri, P.; Peppas, N. A. Mechanisms of Solute Release from Porous Hydrophilic Polymers. *Int. J. Pharm.* **1983**, *15*, 25−35.
(50) Higuchi, T. Rate of Release of Medicaments from Ointment Bases containing Drugs in Suspension. *J. Pharm. Sci.* **1961**, *50*, 874−875.
(51) Hixson, A. W.; Crowell, J. H. Dependence of Reaction Velocity upon Surface and Agitation. *Ind. Eng. Chem.* **1931**, *23*, 923−931.
(52) Kopcha, M.; Lordi, N. G.; Toja, K. J. Evaluation of Release from Selected Thermosoftening Vehicles. *J. Pharm. Pharmacol.* **1991**, *43*, 382−387.
(53) Ritger, P. L.; Peppas, N. A. A Simple Equation for Description of Solute Release. II. Fickian and Anomalous Release from Swellable Devices. *J. Controlled Release* **1987**, *5*, 37−42.

DOI: 10.1021/am508712e
ACS Appl. Mater. Interfaces 2015, 7, 4791−4803